Proceedings of the 2012 IEEE 12th International Conference on Bioinformatics & Bioengineering (BIBE), Larnaca, Cyprus, 11-13 November 2012

Automatic Localization of the Optic Disc in Retinal Fundus Images Using Multiple Features

Touseef Ahmad Qureshi[1], Hassan Amin[2],
Mahfooz Hussain[3], Rashid Jalal Qureshi[4], Bashir Al-Diri[1]
[1]University of Lincoln, Lincoln, UK, [2]NUCES, KPK, Pakistan,
[3]LadyReading Hospital, KPK, Pakistan, [4]University of Debrecen, Hungary
Email: tqureshi@lincoln.ac.uk, baldiri@lincoln.ac.uk, hassan.amin@nu.edu.pk,
mahfoozhussain@hotmail.com, rashidjalal@gmail.com

***Abstract*—Accurate optic disc localization is an essential step for a reliable retinal screening system. Existing methods for the optic disc localization may fail when encountering distractors such as imprecise boundaries, deceptive edge features and inconsistent contrast in retinal images. This paper presents an algorithm (Multi-Scheme method) for localization of the optic disc. The algorithm involves prior domain knowledge such as the optic disc size, cup-to-disc ratio (CDR) and vessel convergence feature to evaluate the confidence level for the candidate region(s) at each thresholding level. Based on the confidence level, the algorithm heuristically decides whether or not to opt for multi-scheme policy for a given image. For optimization, the Computed Response (CR) from variant versions of the same image is calculated in parallel and fits a contour to the optic disc through an iterative process of updating the location of the centre of the contour. The proposed approach has been validated using dataset ONHSD [3] and diaretdb0 [16]; and the results show the robustness and reliability of the proposed method even in the presence of distractors.**

***Index Terms*—Localization, segmentation, optic disc (OD), retinal fundus image, computed response (CR).**

I. Introduction

THIS paper presents a new algorithm for the automatic localization of the optic disc. The algorithm is based on a multi-scheme (scheme 1 and scheme 2) model that roughly locates the real OD through a filtering process which exploits domain knowledge such as the optic disc size, cup-to-disc ratio (CDR) and vessel convergence feature. Candidate regions are associated with confidence level that forms a criterion for switchover between schemes. For optimal localization, the process calculates CR (computed response) by deliberating two versions of the same image in parallel and forms a contour to the optic disc with an optimal location. The two versions of image differ in by the OD features (such as brightness and vessel convergence) focussed in a specific version. We tested our algorithms on ONHSD and diaretdb0 datasets; and presented the result.

A. Motivation

One of the main sign of various retinopathies is the change in the structure of the optic disc in retinal images [6]. Diabetic retinopathy is one of these retinopathies which is the main cause of blindness in working population of developed countries [10]. Furthermore, there is another retinal complication

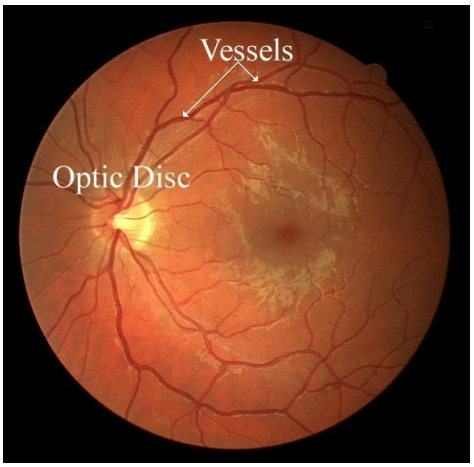

Fig. 1. A retinal image taken from ONHSD database.

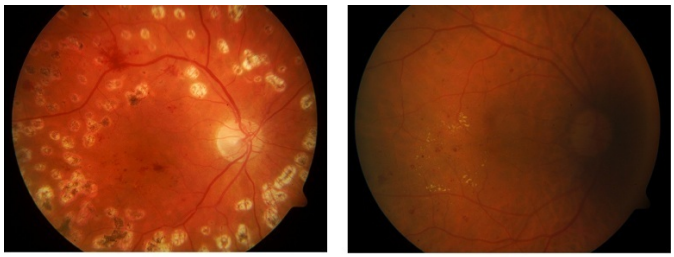

Fig. 2. Retinal images from diaretdb0 database [16] with abnormalities.

glaucoma; a disease increasing worldwide and is expected to reach around 80 million cases in 2020 [5]. All these diseases lead to blindness which can be prevented in at least 60% of cases if proper treatment is given in early stages [3] which involves examining retinal images of patients on regular basis. Examining images for a huge number of patients by only few clinicians is time consuming and prone to errors due to subjectivity. An automated screening system on the other hand will assist the expert for identifying and segmenting retinal components as well as for diagnosing diseases in an efficient, accurate and at substantially low cost.

One of the important tasks for an automated screening system is to accurately locate the optic disc; a bright oval shaped area, responsible for the flow of information from eye to brain [1]. An inevitable task for the automatic system is to differentiate between the optic disc and the retinopathy's symptoms such as tortuous vessels, choroidal neovascularization and exudates which may exist with the same colour intensity, shape and size as the optic disc have, see figure 2(a).

The methodologies to locate the optic disc can be categorized based on the optic disc feature(s) being focussed such as brightness, size, geometrical location, shape, and vessel convergence property. We have proposed a robust and reliable method which heuristically switches between two policies depending on the image appearance. The combination of these policies (named scheme 1 and 2 in our technique) refrains from projecting single attribute of the optic disc during detection process. In particular, scheme 1 establishes the basis on features such as the size and brightness of the OD, on the other hand scheme 2 purely focusses vessel converging feature to locate the OD.

B. Optic Disc Appearance

Analysing the optic disc's appearance is a necessary step for an accurate localization of the optic disc, see figure 3. The optic disc usually appears as a bright, yellowish and oval shape area with the vertical principal axis varies within width 1.8 ± 0.2 mm and height 1.9 ± 0.2 mm [3]. The main blood vessel converges at the same optic disc while the macula is a dark region of size approximately 1.5 mm [11], usually found in the centre of retinal images. The fovea is a tiny area that lies in the centre of macula and is responsible for our central sharpest vision [13] and usually about 2.5 disc diameter away from the centre of the optic disc towards the temporal side [9].

In fundal images, the optic disc appears as the two half of the whole the optic disc rim; temporal and nasal side. The nasal side is usually less bright as compared to temporal side since most of the vessels, which are darker intrinsically, converges at this end, as shown in figure 3. As opposed to nasal side, the temporal side is a bright region, usually contains a 'cup' shape area. The 'cup' is the brightest portion of the optic disc with size often measured in CDR (cup-to-disc ratio) and usually appear below ratio 0.65 [18].

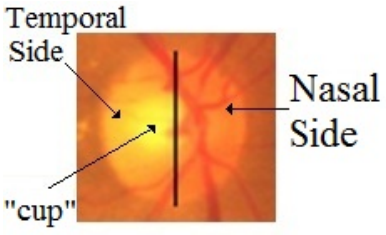

Fig. 3. Typical optic disc where nasal side is darker as compared to temporal side.

In addition, the approximate size of the optic disc in a standard image of healthy retina is one seventh of the whole image [14], see figure 4. The above facts establish a ground while associating confidence level with the candidate OD regions.

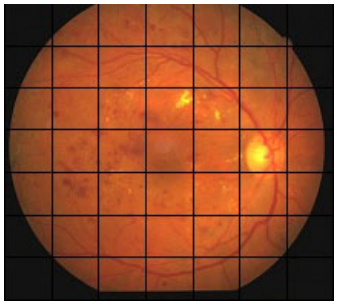

Fig. 4. Optic disc size is almost 1/7th of the entire retinal image.

C. Contents of Paper

This paper is organized as follows. Literature review is discussed is section II, while section III elaborates the methodology for the OD localization (composed of scheme 1 and 2), a relatively simpler technique and less prone to the false OD; and methodology for the optimization that forms an approximate real OD's boundary. Experiments and results are discussed in Section IV whereas the Section V concludes the paper.

II. Backround

One of the primary features to localize the optic disc or at least to identify the region of interest is blood vessels. Vessels may be characterized by the expected color (reddish), shape (curvilinear), gradient (strength of boundary), and contrast (with background) [2], See figure 1. Vessel convergence (vessels radiate from the optic nerve head) and vessel density has been used to detect the optic disc. Akita and Kuga localized the optic disc by backtracking the blood vessel to the optic disc [8] while S Ravishankar et al. proposed a method in which only the major (thicker) blood vessel is considered [15]. The techniques which purely based on vessel convergence property, suffer difficulties in low contrast images or when vessels are hardly visible.

Brightness is another genuine attribute of the optic disc supported several localization techniques. Liu et al [17] formed clusters of the pixels with high intensity in the entire retinal image; out of these, the largest cluster of pixels is taken as the optic disc. Huiqi Li [7] took step ahead by combining the clustering and Principal Component Analysis (PCA) technique to locate the optic disc. In many cases, the largest cluster of pixels may not belong to the optic disc thus contributing to incorrect classification, especially when exudates exists, see figure 2(a).

Few other characteristics such as shape (nearly oval) and colour (highly intensive yellowish) of the optic disc were used in localization techniques. Barrett et al [12] used Hough transform to locate the optic disc and estimated circular shape with fixed radius. S.Sekhar et al [11] used both the colour and

shape property to localize the optic disc by computing the grey tone image of the original retinal image in order to have a good variation between the optic disc and the background. These techniques work well when OD-Background contrast is sufficiently high and the optic disc bears the shape (oval) with strong boundary. However, these techniques might fail when the optic disc is too dull or abnormalities such as circular shaped object exists, see figure 2(a) and 2(b).

A combination of several image processing techniques might increase the performance to locate the real optic disc. Balazs et al [4] combined previously discussed techniques based on multiple properties of retinal images. Their algorithm is basically a fusion of five segmentation techniques; Pyramidal Decomposition, Edge Detection, Entropy Filter, Fuzzy Model and Hough transformation. M. Lalonde et al [9] used the confidence level after applying Pyramidal decomposition and Hausdorff-based template matching techniques. A. Hunter et al [3] localized the optic disc using specialized template matching and then segmented OD using a deformable model with variable edge-strength dependent stiffness.

Localization of the optic disc is a multi-faceted problem which is further complicated in case of non-healthy retinal images due to the presence of various kinds of disease symptoms. There is a clear threat for the techniques that based on single attribute of the OD. On the other hand a domain specific technique is required which incorporates prior knowledge of attributes of the optic disc, blends localization techniques and create a model which can associate confidence level with the optic disc candidates.

We propose a two-step localization model which not only composes of multi-attributes of the optic disc, but possess a heuristic nature (multi-scheme concept) at the same time. The proposed model analyses and selects the most suitable attribute of the optic disc to be focussed for the given image. In the first step, we use simple thresholding to get the candidate(s) OD, which are then associated with confidence level through evaluating their sizes by comparing with an average optic disc size and vessels convergence response at each candidate OD. The candidate OD with highest confidence level is considered the true OD candidate. In the second step, we form a contour that moves based on the response from both the grey level image and binary image of segmented vessels, to get optimization for local fitting.

III. Methodology

A. Screening Data

We have tested the algorithms on the dataset used by A. Hunter in [3]. The dataset consists of 99 fundal images taken from 50 patients at City Hospital, Birmingham and is available on our official site http://reviewdb.lincoln.ac.uk/. The patients from various ethnic backgrounds with mean age 63.7 (s.d 14.8 years) were included in the screening program. All images were acquired using canon's camera CR6 45MNf (field angle lens = 45 degree) with resolution 640x480. The complete description of the dataset is available in [3]. We have implemented the technique on diaretdb0 dataset [16] as well that contains 130 retinal images with a variety of retinopathies.

B. Automatic Localization of the Optic Disc

The technique exploits the multiple characteristics associated with the OD in a cascaded fashion, avoiding the temptation of the false ODs and drawing the real OD selection through filtering process. The key objective is to heuristically decide about the use of a certain OD attribute for a given image. For a coherent understanding, both the schemes will be discussed separately; however before a formal discussion on technique, we calculate values for few variables used in the proposed technique.

The 'cup' area, which has been mostly presumed the brightest area, forms a foundation for switchover criteria. We calculate the approximate 'cup' area (we call it $|\gamma|$) for a given image of arbitrary resolution using CDR and a single block's measurement (which is equal to an average optic disc size, see figure 5), by dividing the image in to 7 equal rows and columns. Mathematically by

$$|\gamma| = [(ymax)(xmax)](CDR) \quad (1)$$

Whereas $ymax$ and $xmax$ are the maximum width and height of one block, see figure 5).

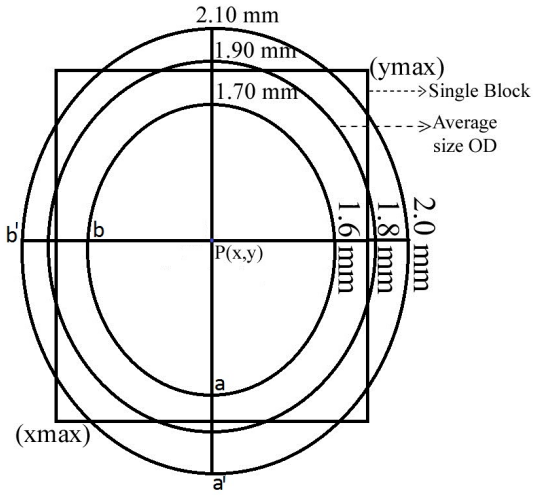

Fig. 5. The size range of the optic disc with the proportion of a single block (after 7x7 division) of a retinal image.

In addition, we assume that the pixels belonging to 'cup' area having higher intensity than the middle grey level; this assumption forms a criteria for switching to scheme 2.

Moreover, to calculate computed response (CR) for a particular pixel (p) at location (x, y), we take the binary segmented image for vessels by applying the Laplacian of Gaussian (LoG) edge detector on the original image (I), mathematically by:

$$LoG(I(x,y)) = \left[\left(\frac{x^2+y^2-2\sigma^2}{\sigma^4}\right) e^{-\frac{x^2+y^2}{2\sigma^2}} \right] (I(x,y)) \quad (2)$$

We implemented the matlab function for LoG edge detector with $\sigma = 2$.

And then calculate the Computed Response (CR) by counting the number of white pixels within the area with $xmax$ as height, $ymax$ as width and p as a central point, see figure 5, mathematically by:

$$CR = \sum_{i=1}^{xmax} \sum_{j=1}^{ymax} I_{logfr}(i,j) \tag{3}$$

Here I_{logfr} denotes focal region (region of interest) after LoG transform while $xmax$ and $ymax$ are the maximum vertical and horizantal respective pixels in focal area. The maximum and average value of CR is calculated for later use and kept in variable (N) and (O) respectively. The working of the whole system is shown in figure 6, comprised of localization (scheme 1 and scheme 2 block) that eventually leads to optimization block.

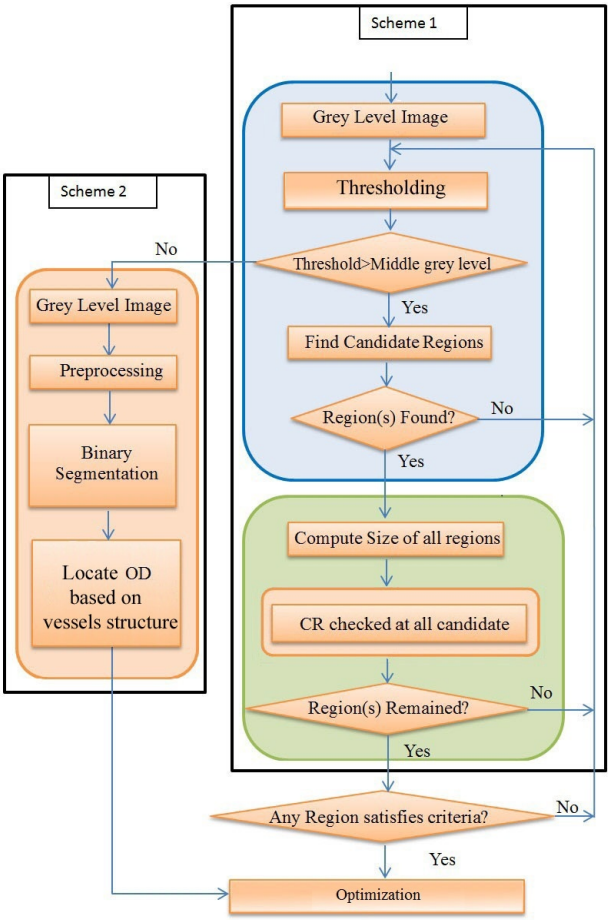

Fig. 6. Organization of the entire system explaning the order of steps for localization

1) Scheme 1: We take the grey level image (I_g) and design a thresholding model which keeps three parameters in to account, i.e. maximum grey level of a given image $(gmax)$, middle grey level$(gmid)$, and the 'cup' size$(|\gamma|)$. The threshold (T) starts from maximum grey level and keeps on decreasing by one level while seeking for the candidate OD regions at each level, see figure 7.

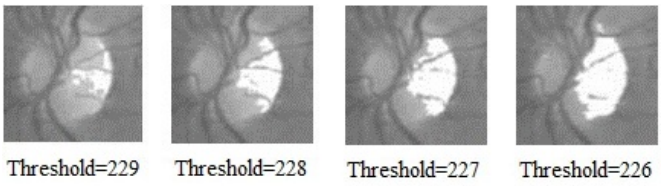

Fig. 7. Discovering most suitable threshold.

At each level, after obtaining the candidate OD region(s), the size of each candidate OD region is compared with the standard 'cup' size, mathematically by

begin
  $T = gmax$
  while $(T \geq gmid)$
    if $(R \geq |\gamma|)$ for every R
      Candidate OD found
    else
      $T = T - 1$
    end
  end
end

Where as R is the region(s) found after a specific T. Provided the system finds a candidate region(s) greater or equal to size of 'cup', it proceeds to evaluating the confidence level of a particular region by taking the central point of the candidate region, calculating the CR for that point (M), and comparing it the highest CR of the image, i.e. (N). The less difference between (M) and (N), the higher the probability is for candidate region to be the true OD and vice versa. The system kept associating the value M with candidate region(s) till the threshold (T) reaches the middle grey level. The system selects the candidate region with highest CR as the true OD area, provided there is no region with CR less than the average CR (O), mathematically by:

$$Switchover\ if\ (T < gmid) AND (M < O) \tag{4}$$

2) Scheme 2: The 'shift to scheme 2' is a heuristic decision against the reliability of the 'OD brightness' as localizing feature; i.e. it testifies the presence of the OD with low illumination or even a complete absence of the OD in the image. The pre-processing step implicates applying a median filter to produce a noise free image; we have used a mask of size 10x10 (10 Percent of the average optic disc size for image of any size). We have used the binary segmented image for vessels (I_{logfr}), see figure 8 and morphological closing(8-connected pixels) is used to bridge the gap between vessels breakups, given by equation below.

$$A \bullet B = (A \oplus B) \ominus B \tag{5}$$

Where as $\bullet$, $\oplus$ and $\ominus$ sign is used for morphological closing, dilation and erosion respectively. See figure 8 shows an example of binary segmentation of vessels.

Each pixel of the image is associated with a CR calculated by taking the focused pixel as centre of area equals to the

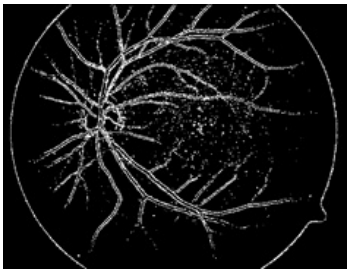

Fig. 8. Vessel extraction after applying LoG edge detection and morphological closing.

average optic disc size. The pixel with highest CR gives approximate centre of the true OD.

3) Optimal Localization (Optimizaion): After localizing the approximate center of the OD (Obtained from Scheme 1 or 2); our approach attempts to form a contour that fits the boundary of the OD using the average OD size. The position of the contour is updated by iteratively changing the center of contour within focal area (between a and $a^{'}$, and b and $b^{'}$) to get the maximum response based on the OD's local features. The boundary may also shrink or expand within the limits defined for optimization.

The response from two versions of image, i.e. grey level (I_g) image and image obtained after binary segmentation of vessels using LoG (I_{logfr}), are integrated to estimate for an overall optimal response (R_v). In particular, the intensity count from grey level image R_1 and vessels response (Vessel's quantity or R_2) from binary segmented image of vessels is based, mathematically given by:

$$R_v = R_1 + R_2 \tag{6}$$

where as

$$R_1 = \sum_{i=1}^{xmax} \sum_{j=1}^{ymax} I_{gfr}(i,j) \tag{7}$$

and

$$R_2 = \sum_{i=1}^{xmax} \sum_{j=1}^{ymax} I_{logfr}(i,j) \tag{8}$$

Here, I_{gfr} denotes grey level focal region while I_{logfr} represents focal region after Laplacian of Gaussian transform.

IV. Results and Discussion

The performance of the technique is assessed in two phases; i.e. detection or localization phase, and optimization phase. Experiments proved the earlier phase's robustness and reliability while a minor compromise associated with the later one. The technique has been implemented on Matlab(r)(version 7.10, R2010a) and outcomes are examined at every major step. The three major breaks considered are scheme 1's outcome, scheme 2 call and outcome, and finally the optimization's phase outcome. We have tested our algorithm on ONHSD and diaretdb0 database, compared the technique and presenting the following statistics.

Localization is considered successful even if there is a very small intersection between the obtained and the true OD's area. We got 100% true localization on all useable images of ONHSD and with a very few calls to scheme 2. There were two non-useable images that ended up in false-positive cases. In case of diaretdb0, we got 98.4% true localization with a couple of calls to scheme 2. The result proves the algorithm's consistency and promising behaviour in spite of distractors present in the image.

Although the localization algorithm has revealed the ability to seize major part of the OD in most of the cases; the optimization on the other hand takes multiple versions of the image in parallel and calculates optimal response from corresponding areas for local fitting. To evaluate the performance of the optimization phase, we manually selected the central point of the optic disc in all images of the two datasets and analysed how far the manually selected central point is from the central point obtained from the proposed method (localization and optimization). We classified optimization result in to four levels, i.e. *d1* through *d4* based on the distance from central point, see figure 9.

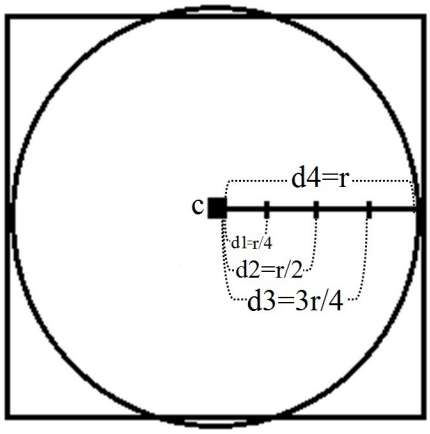

Fig. 9. Single block after dividing the retinal image in to seven equal parts; covering an average size optic disc with *c* as central point and *r* as radius. The measurements *d1=r/4, d2=r/2, d3=3r/4* and *d4=r* are the distances from the point *c*.

The result is considered 'Excellent' in case the distance between the manually selected central point and obtained central point from the proposed method is not greater than the value of *d1*. Similarly *d2* represents 'Good' optimization, while *d3* and *d4* represents 'Fair' and 'Poor' optimization respectively. The following table (Table 1) shows the result of the optimization phase.

TABLE I
The Results after Optimization Process

Data Set	No of Images	Excellent	Good	Fair	Poor
ONHSD	97	94.8	3.0	0	2.06
diaretdb0	128	93.75	4.6	1.56	0

The 'No of Images' in the table represents the total number

of cases in which the true optic disc is detected in the localization step. In addition, the table shows the optimization process yielded in '*d1*: Excellent' class in 94.8% of images of ONHSD and 93.75% in case of diaretdb0, proclaiming the stability of technique. The 'Good' and 'Fair' class consists not more than 5% of the images in both the cases of ONHSD and diaretdb0. The analysis of 'poor' class cases manifests the advert effect due to poor vessel edges or increase in the OD size due to glaucoma, see figure 10.

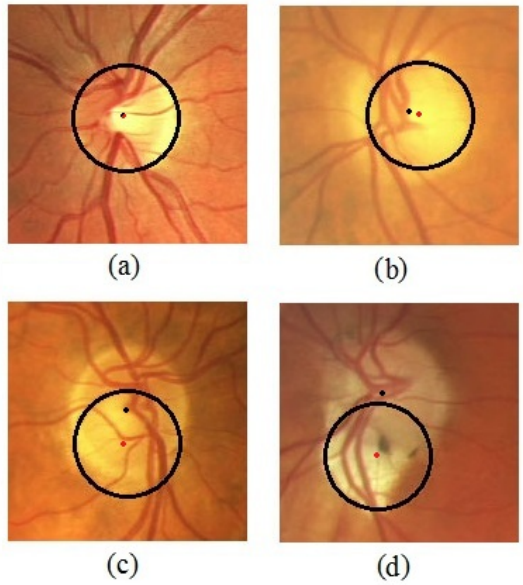

Fig. 10. The black dots represent gold standard and red dots represent the centre of the obtained optic disc's boundary. a:Excellent, b:Good, c:Fair and d:Poor.

V. Conclusion and Future Work

Automatic detection of retinal components is a necessary step for a screening system. In our proposed approach we tried to overcome the limitations found in other techniques. The proposed approach tried not to stick only on a single property (i.e. colour/intensity, shape and vessels), but used multiple properties where needed to get optimal result. The proposed approach comprise of two steps, i.e. Localization and optimization. The optic disc Localization is achieved using a relatively simple technique of thresholding to get desired cluster based on prior knowledge such as the average optic disc size and CDR; and dynamically selected intensity range where it may be found. The technique heuristically decides regarding focused attribute to form basis on, and incorporate alternate scheme if needed. In addition, the second part of technique uses CR from multiple versions of the same image and updates the location of the formed contour over the OD boundary to get an optimal localization. The technique has worked well and offers promising performance for other more difficult datasets. We intend to reform our localization model in future by taking shape attribute in account to get more reliability and improvement.

References

[1] A. Hoover and M. H. Goldbaum, "Locating the optical nerve in a retinal image using the fuzzy convergence of the blood vessels," IEEE Trans. Med. Imag., vol. 22, no. 8, pp. 951-958, 2003.

[2] A. Hoover, V. Kouznetsova, and M. H. Goldbaum, "Locating blood vessels in retinal images by piece-wise threshold probing of a matched filter response," IEEE Trans. Med. Imag., vol. 19, no. 3, pp. 203-210, 2000.

[3] A. Hunter, J. Lowell, D. Steel, A. Basu, R. Ryder, E. Fletcher, and L. Kennedy, "Optic nerve head segmentation," IEEE Trans. Med. Imag., vol. 23, pp. 256-264, USA.

[4] B. Harangi, R. J. Qureshi, A. Csutak, T. Peto, and A. Hajdu, "Automatic detection of the optic disc using majority voting in a collection of optic disc detectors," IEEE International Symposium on Biomedical Imaging (ISBI), pp. 1329-1332, 2010.

[5] H. A. Quigley and A. T. Broman, "The number of people with glaucoma worldwide in 2010 and 2020," Br. J. Ophthalmol., vol. 90, no. 3, pp. 262-267, 2006.

[6] H. Li and O. Chutatape, "Automated feature extraction in color retinal images by a model based approach," IEEE Trans. Biomed. Eng., vol. 51, pp. 246-254, 2004.

[7] H. Li and O. Chutatape, "Automatic location of optic disk in retinal images," in Proc. IEEE-ICIP, pp. 837-840, 2001.

[8] K. Akita and H. Kuga, "A computer method of understanding ocular fundus images," Pattern Recogn., vol. 15, no. 6, pp. 431-443, 1982.

[9] M. Lalonde, M. Beaulieu, and L. Gagnon, "Fast and robust optic disc detection using pyramidal decomposition and hausdorff-based template matching," IEEE Trans. Med. Imag., vol. 20, no. 11, pp. 1193-1200, 2001.

[10] A. Aquino, M. E. Gegundez-Arias, and D. Marin, "Detecting the optic disc boundary in digital fundus images using morphological, edge detection, and feature extraction techniques," IEEE Trans. Med. Imag., vol. 29, pp. 1860-1869, 2010.

[11] S. Sekhar, W. Al-Nuaimy, and A. K. Nandi, "Automated localization of optic disk and fovea in retinal fundus images," European Signal Processing Conference (EUSIPCO), August 25-29, 2008.

[12] S. Barrett, E. Naess, and T. Molvik, "Employing the hough transform to locate the optic disk," Biomed. Sci. Instrum., vol. 37, pp. 81-86, 2001.

[13] S. Chaudhuri, S. Chatterjee, N. Katz, M. Nelson, and M. Goldbaum, "Detection of blood vessels in retinal images using two-dimensional matched filters," IEEE Trans. Med. Imag., vol. 8, no. 3, pp. 263-269, 1989.

[14] S. Liu and J. Chen, "Detection of the optic disc on retinal fluorescein angiograms," J. Med. Biol. Eng., vol. 31, no. 6, pp. 405-412, 2011.

[15] S. Ravishankar, A. Jain, and A. Mittal, "Automated feature extraction for early detection of diabetic retinopathy in fundus images," IEEE Conf. Comput. Vis. Pattern Recognit., pp. 210-217, 2009.

[16] T. Kauppi, V. Kalesnykiene, J-K. Kamarainen, L. Lensu, I. Sorri, A. Raninen, R. Voutilainen, H. Uusitalo, H. Klviinen, and J. Pietil, "DIARETDB1 diabetic retinopathy database and evaluation protocol," Proc. Medical Image Understanding and Analysis (MIUA), pp. 61-65, 2007.

[17] Z. Liu, C. Opas, and S. M. Krishnan, "Automatic image analysis of fundus photograph," Proc. 19th Annu. Int. Conf. IEEE Engineering in Medicine and Biology Society (EMBS), vol. 2, pp. 524-525, 1997.

[18] Z. Zhang, J. Liu, W. Kee, N. M. Tan, J. H. Lim, S. Lu, H. Li, Z. Liang, and T. Y. Wong, "Neuro-retinal optic cup detection in glaucoma diagnosis," Biomedical Engineering and Informatics (BMEI), 2009.